Detrital illite crystals identified from crystallite thickness measurements in siliciclastic sediments

LUCA ALDEGA[1],* AND D.D. EBERL[2]

[1]Dipartimento di Scienze Geologiche, Università degli Studi "Roma Tre", Largo S. L. Murialdo 1, 00146 Roma, Italy
[2]U. S. Geological Survey, 3215 Marine St., Suite E-127, Boulder, Colorado 80303, U.S.A.

ABSTRACT

Illite crystals in siliciclastic sediments are heterogeneous assemblages of detrital material coming from various source rocks and, at paleotemperatures >70 °C, of superimposed diagenetic modification in the parent sediment. We distinguished the relative proportions of $2M_1$ detrital illite and possible diagenetic $1M_d + 1M$ illite by a combined analysis of crystal-size distribution and illite polytype quantification. We found that the proportions of $1M_d + 1M$ and $2M_1$ illite could be determined from crystallite thickness measurements (BWA method, using the MudMaster program) by unmixing measured crystallite thickness distributions using theoretical and calculated log-normal and/or asymptotic distributions. The end-member components that we used to unmix the measured distributions were three asymptotic-shaped distributions (assumed to be the diagenetic component of the mixture, the $1M_d + 1M$ polytypes) calculated using the Galoper program (Phase A was simulated using 500 crystals per cycle of nucleation and growth, Phase B = 333/cycle, and Phase C = 250/cycle), and one theoretical log-normal distribution (Phase D, assumed to approximate the detrital $2M_1$ component of the mixture). In addition, quantitative polytype analysis was carried out using the RockJock software for comparison. The two techniques gave comparable results ($r^2 = 0.93$), which indicates that the unmixing method permits one to calculate the proportion of illite polytypes and, therefore, the proportion of $2M_1$ detrital illite, from crystallite thickness measurements. The overall illite crystallite thicknesses in the samples were found to be a function of the relative proportions of thick $2M_1$ and thin $1M_d + 1M$ illite. The percentage of illite layers in I-S mixed layers correlates with the mean crystallite thickness of the $1M_d + 1M$ polytypes, indicating that these polytypes, rather than the $2M_1$ polytype, participate in I-S mixed layering.

INTRODUCTION

Clay minerals contained in shale and sandstones undergo diagenetic and very low-grade metamorphic reactions when sedimentary basins subside in response to burial and/or tectonic loading. Reactions in clay minerals are irreversible under normal diagenetic and anchizonal conditions, so that uplifted and exhumed sequences generally retain indices and fabrics indicative of maximum maturity and burial (Árkai 2002; Árkai et al. 2002). Clay minerals are mainly sensitive to temperature, and the use of illite-smectite (I-S) mixed layers as a "geothermometer" is generally accepted (Burst 1959; Hower et al. 1976; Pollastro 1990). In fact, changes in the composition of mixed layering, layer expandability, and I-S ordering (as interpreted from X-ray powder diffraction profiles) are empirically related to temperature changes due to burial (Hoffman and Hower 1979; Pollastro and Barker 1986; Botti et al. 2004). Nevertheless, other factors (e.g., heating rate, protolith, fluid composition, permeability, fluid flow) may control the illite enrichment of I-S mixed layers (Roberson and Lahann 1981; Colten-Bradley 1987; Pytte and Reynolds 1989; Hartmann et al. 1999).

Illite crystals in siliciclastic sediments in fold and thrust belt settings are heterogeneous assemblages of detrital material coming from various source rocks, and, at paleotemperatures >70

°C (Merriman and Kemp 1996), of superimposed diagenetic modifications of this sediment. Only diagenetic rather than detrital phases should be used to estimate paleotemperatures and to constrain the burial history of folded and thrust sedimentary successions that range in alteration intensity from diagenesis to low-grade metamorphism. In fact, detrital illite only records environments inherited from the past, generally of higher temperature, not directly related to the burial history of the sedimentary successions. Furthermore, in hydrocarbon exploration, illite studies are used to calibrate the heating history of sedimentary basin to ascertain that oil or gas generation from source rocks postdated trap formation (Peaver 1999). Hence, the extraction of quantitative information that distinguishes diagenetic illite from detrital micas is a great challenge for many clay mineral researchers.

Separation of detrital and authigenic illite crystals can be obtained by gravity separation in distilled water followed by ultracentrifugation. These grain-size separations can be improved by high-grade magnetic separations that permit the separation of authigenic, non-magnetic illite from detrital, more-magnetic micas that have the same particle size (Tellier et al. 1988). K-Ar dating of different grain-size fractions also can be interpreted to identify detrital and diagenetic phases (Peaver 1999). Other studies aimed at the same goal have been performed, for example, by Uhlik et al. (2000), who investigated the thickness distribution of illite crystals in diagenetically altered shales using

---

* E-mail: aldega@uniroma3.it

high-resolution transmission electron microscopy (HRTEM) on PVP-10-intercalated illite-smectite samples. Dudek and Środoń (2003) modeled asymptotic illite thickness distributions using a number of theoretical log-normal distributions in order to identify and quantify I-S and discrete illite phases in shales.

Another way to distinguish diagenetic and detrital illite is a combined analysis of crystal-size distributions and illite poly-types quantification. The present paper describes a new method for calculating the proportion of detrital and diagenetic illite from crystallite thickness measurements using the MudMaster computer program of Eberl et al. (1996) based on the X-ray diffraction technique of Bertaut-Warren-Averbach (BWA; Drits et al. 1998). The results were checked by quantitative XRD analysis of illite polytypes performed using the Rockjock software (Środoń et al. 2001; Eberl 2003).

BACKGROUND GEOLOGY

The Northern Apennines can be described as a mountain chain made up of structural units and nappes accreted onto the Adriatic Foreland (Fig. 1). The Ligurian Nappe is the uppermost structural unit. It represents remnants of the oceanic Alpine Tethys and comprises an association of ophiolite bearing-rocks, mudstones, and deep-water turbidites and a Subligurian succession deposited on the thinned continental crust of the Adriatic margin. The Ligurian Unit overthrust a series of structural units (Tuscan,

Modino, Cervarola Unit, and Umbria-Marche Domain) derived from the deformation of the western Adriatic continental margin. These units contain stratigraphic sequences made of Mesozoic evaporitic and carbonate deposits covered by Oligocene to Miocene turbidite deposits, which are progressively younger toward the northeast. The main turbiditic successions are known as the upper Oligocene to lower Miocene Macigno (Tuscan Unit), the lower Miocene Modino sandstone (Modino Unit), the lower-middle Miocene Cervarola sandstone (Cervarola Unit), and the middle-upper Miocene Marnoso-Arenacea Formation (Umbria-Marche Domain).

The study area represents the core of the Modena-Bologna segment of the Northern Apennines fold and thrust belt in which the Cervarola Unit outcrops. This structural unit contains two turbidite successions tectonically stacked on top of each other and traditionally known as the Cervarola sandstones (Burdigalian) and the Granaglione sandstones (Langhian). After the thrusting of the Cervarola sandstones over the Granaglione sandstones in post-Langhian times, four thrust sheets developed deforming the latter turbiditic succession. The geometrical relationship between the Cervarola and Granaglione sandstones is shown in Figure 2.

Apart from large outcrops of metamorphic rocks well exposed in Tuscany, most of the rocks of the Northern Apennines reached only diagenetic conditions. Existing data from the investigated
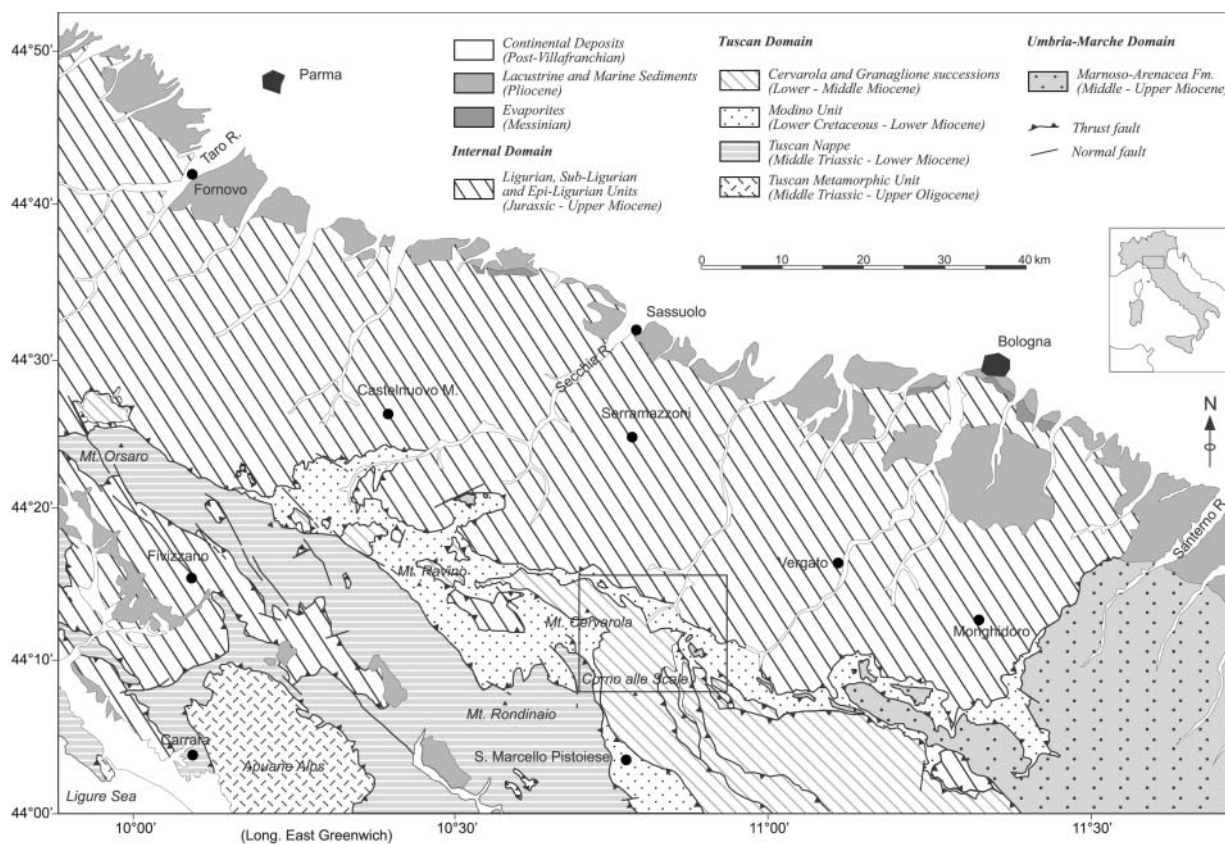

FIGURE 1. Geological sketch map of the Northern Apennines, compiled after Boccaletti (1982) and Plesi et al. (2002). Box shows the study area.
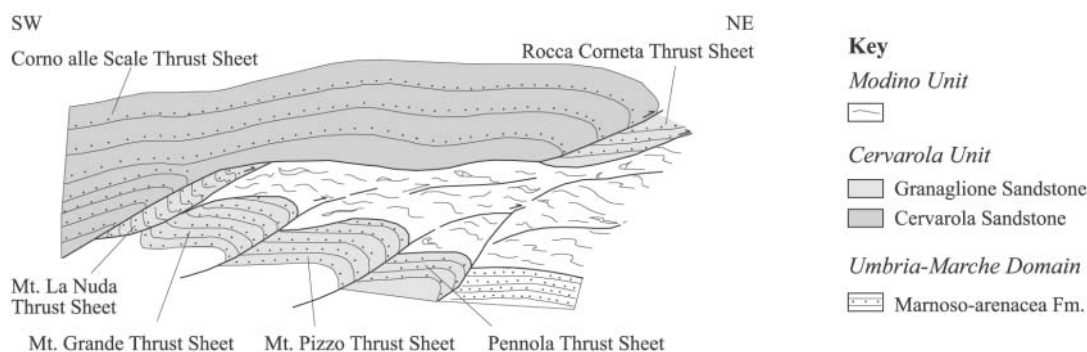
FIGURE 2. Present day reconstructed geometrical relationships between the Cervarola and the Granaglione sandstones outcropping in the study area. Distances are not to scale.

zone and the surrounding areas on the metamorphic grade of the studied successions come from organic matter maturity and clay mineralogy. Reutter et al. (1980, 1991) showed a general decrease of Ro values from the internal toward the external zones and through the nappes from the lowermost to the uppermost unit from 2.4% to 1.0%. Botti et al. (2004) recognized a similar trend in the Granaglione sandstones and pointed out a horizontal decreasing maturity trend from the inner (Mt. La Nuda thrust sheet) to the outer (Pennola thrust sheet) thrust sheet from 1.54% to 1.35%. In addition, these authors indicated an increase of thermal maturity from the younger to the older sediments in the studied successions. Ro% values range from 1.01% to 1.2% and the illitic content in the illite/smectite (I-S) mixed layers slightly increases from 80% to 90%.

A suite of 21 samples was collected for crystallite thickness measurements and polytype analysis, mainly from the stratigraphic succession in the upper thrust sheet of the Cervarola sandstones (12 samples distributed in a ~2000 m thick succession) and from the four lower thrust sheets in the Granaglione sandstones (9 samples distributed in a ~600 m thick succession; Fig. 3). Samples were collected mainly from the Tc and Td intervals of the Bouma division of thin-fine turbiditic beds and black shales (RU1V-RU3V).

SELECTION OF STUDY AREA

This sector of the Northern Apennines represents a key area where one can test the effectiveness of the proposed methodology. First, the studied successions are well exposed and a detailed sampling strategy could be performed.

Second, a large input of $1M_d$ + $1M$ illites originating from diagenetic rocks eroded in the source area can be excluded.

A recent paper by Botti et al. (2004) on the integrated use of both organic matter maturity and clay mineralogy reconstructed the burial history of the Cervarola and Granaglione sandstones and their tectonic evolution since Aquitanian times. A calculated tectonic loading of 3.5 km and of ~5.0 km on the Cervarola and Granaglione sandstones, respectively, has been indicated as the main factor responsible for the acquired thermal maturity of the studied area. The emplacement of the allochtonous units on these sediments took place almost simultaneously after the deposition of the Cervarola Unit, terminating its sedimentation history and preserving it from erosion.
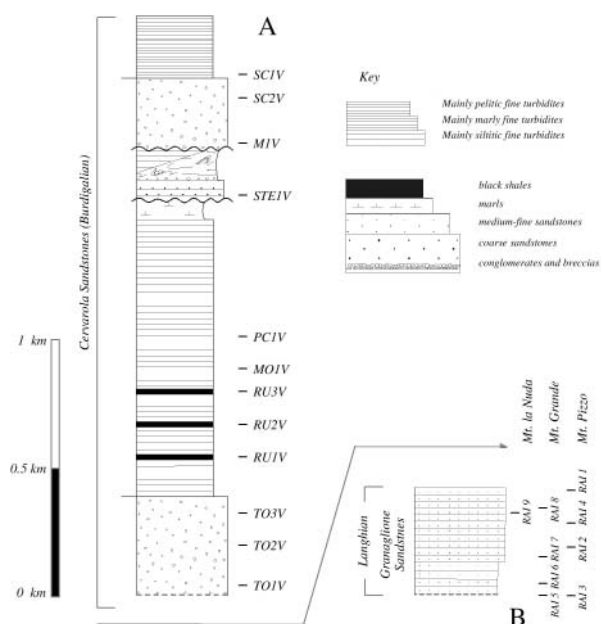

FIGURE 3. Synthetic stratigraphic logs of the Cervarola sandstones (A) and Granaglione sandstones (B) with sample location.

METHODS

Samples were lightly crushed and disaggregated in distilled water with an ultrasonic probe. Then Na-saturated whole-rock samples, <0.2 μm (equivalent spherical diameter) and <2 μm grain-size fractions were intercalated with a polymer, polyvinilpyrrolidone (hereafter PVP-10), and X-rayed on a single crystal Si-wafer according to Eberl et al. (1998).

Samples were analyzed in Boulder, Colorado, using a Siemens D500 XRD system with a graphite monochromator, Cu$K\alpha$ radiation, and a scintillation counter. Samples generally were scanned from 3 to 10 °2θ with a step size of 0.02 °2θ and a count time of 20 s per step. Only samples from the Granaglione sandstone were scanned with a lower count time of 5 s per step. The tube current and the voltage were 30 mA and 40 kV, respectively.

The intensities of the 10 Å X-ray diffraction peaks were corrected for the combined broadening effects of the Lorentz-polarization (Lp) function and the layer scattering intensity G^2 (square of the structure factor) using the default values for these parameters found in the MudMaster program. Then, following background subtraction and optional removal of the contribution of the $K\alpha_2$ radiation, a Fourier analysis of the interference function was undertaken using the BWA approach to calculate the distribution of thicknesses of X-ray diffraction domains (Eberl et al. 1996).

Although the options are included in the program, removal of the $K\alpha_2$ radiation

and correction for instrumental broadening were not performed, because such corrections are unnecessary in our experimental setup if the crystallite thickness is less than about 20 nm, and if 2θ for the peak is less than about 50° (Eberl et al. 1996; Kotarba and Środoń 2000). In addition, it was found that the effects of changes in K and Fe content on the layer scattering intensity for illite crystals and the effect of changing crystallite orientation on the Lp factor do not significantly affect the values calculated for crystallite thickness (e.g., Eberl et al. 2003).

Adjacent reflections that overlap within the range of analysis (e.g., the 001 chlorite peak) were removed using the PeakChopper tool supplied with the MudMaster program. Calculations have shown that this method of peak removal does not introduce error into the MudMaster analyses (Eberl et al. 2003).

Quantitative XRD polytype analysis was carried out using RockJock software (Środoń et al. 2001; Eberl 2003) on randomly oriented sample mounts prepared by side-loading a sample holder that accommodates approximately 600 mg of clay. Samples were X-rayed from 5 to 65 °2θ with a step size of 0.02 °2θ and a count time of 5 s per step at 40 kV and 30 mA. Samples were analyzed using RkJock3.xls and the full pattern method, with automatic shifts in the 2θ positions of the illite standards to approximate isomorphous substitutions in the samples that differed in composition from the standards. RockJock calculates the wt% minerals in samples by comparing the integrated X-ray diffraction intensities of individual minerals in complex mixtures to the intensities of an internal standard (ZnO). The program fits the sum of stored XRD patterns of standards (calculated pattern) to the measured pattern by varying the fraction of each standard pattern. This is achieved by using the Solver function in Excel to minimize the degree of fit parameter between the calculated and measured pattern.

Qualitative identification and quantification of illite-smectite mixed layers was performed in Rome with a Scintag X$_1$ XRD system (Cu$K\alpha$ radiation, solid state detector, spinner). Oriented air-dried samples were scanned from 1 to 48° 2θ with a step size of 0.05° 2θ and a count time of 4 s per step at 40 kV and 45 mA. The presence of expandable clays was determined for samples treated with ethylene glycol at 25 °C for 15 h. Ethylene-glycol solvated samples were scanned under the same conditions as air-dried aggregates with a scanning interval of 1–30 °2θ. Expandability measurements were determined according to Moore and Reynolds (1997) using the Δ2θ method after decomposing the composite peaks between 9–10 °2θ and 16–17 °2θ using the Scintag X1 software program with a split Pearson VII function.

POLYTYPE ANALYSIS

Polytypes are a variety of two-dimensional polymorph distinguished by various stacking arrangements of identical layers. The 2M$_1$ polytype is expected for the large detrital micas eroded from slates, schists, and phyllites and the 1M polytype grows in bentonites and sandstones (Peaver 1999). 1M$_d$ illite also may grow in shales, or may result from deposition. These observations indicate that the 1M (and possibly the 1M$_d$) material mixed with 2M$_1$ illite in shales and siltites is often diagenetic, whereas the 2M$_1$ micas generally are detrital. Standard patterns for illite 1M$_d$, 1M, and 2M$_1$ polytypes were represented by the pure illites PDU, RM30, and SG4 (Eberl et al. 1987), respectively. We extracted

the wt% of each polytype from all the identified minerals, then normalized it to 1.0. General quantitative mineralogy for selected samples are given in Table 1. Normalized polytype results are shown in Table 2. A lack of discrete smectite and the presence of only trace amounts of kaolinite indicate that superficial (or shallow) weathering may have been unimportant.

CRYSTALLITE-THICKNESS DATA

Illite crystallite thickness distributions (CTD) measured by XRD for <0.2 μm (equivalent spherical diameter), <2 μm grain-size fractions, and whole-rock samples are given in Table 3 and shown in Figure 4 (frequencies normalized to 1.0). The samples are arranged according to the stratigraphic sequence. Measurements of the 001 peak yielded two main types of crystal size distribution shapes, asymptotic and log-normal. Asymptotic-like distributions deviate from log-normality because of the large number of 2 nm crystals. Log-normal distribution measurements are characterized by a spike at 2 nm that is considered to be an artifact of the hook correction performed in the MudMaster program (Brime and Eberl 2002; Eberl et al. 2003). The program is optimized to reproduce the asymptotic distribution rather than the log-normal shape. Hence, the spikes were removed from log-normal CTDs measured for RU samples by using a smoothing power of 1 in the MudMaster analysis. Samples with log-normal CTDs are black shales whereas the asymptotic shapes correspond to siltites.

Samples SC1V, SC2V, and M1V have a greater mean size than the samples below. These samples contain greater amounts of 2M$_1$ (detrital) illite (Table 1). In addition, the general shapes of the area-weighted thickness distributions were the same for each size fraction, indicating that approximately the same population of illite crystals was found in each fraction. The major difference between size fractions is the increase of the 2 nm thickness class in the <0.2 μm grain-size fraction, suggesting the presence of more diagenetic illite crystallites in the finest size fractions.

ILLITE-SMECTITE RESULTS

Illite-smectite mixed layers (I-S) observed in the <2 μm grain-size fraction correspond to R > 1 structures wherein the illite content ranges between 80% and 90% (Table 4 and Fig.

TABLE 1. Quantitative XRD analyses of selected samples using RockJock

| Sample	SC1V	SC2V	M1V	STE1V	PC1V	MO1V	RU3	RU2	RU1	TO3V	TO2V	TO1V
Degree of fit	0.093	0.083	0.108	0.142	0.113	0.093	0.080	0.081	0.073	0.103	0.085	0.086
Non-clay minerals												
quartz	22.5	26.1	22.9	14.1	30.5	34.9	17.0	13.1	15.5	28.4	27.1	30.6
microcline	2.1	2.8	2.0	0.5	1.7	2.3	0.5	1.5	0.8	3.3	4.0	3.0
orthoclase	0.5	2.2	0.8	1.1	2.0	1.9	0.4	0.0	0.3	1.6	1.2	1.1
albite	11.5	20.0	16.8	6.5	15.8	16.8	0.7	0.6	1.2	22.1	15.1	12.1
calcite	18.9	14.5	8.7	47.3	21.3	15.9	0.0	1.1	1.4	6.6	7.0	12.9
dolomite	1.9	3.0	3.4	0.9	3.0	3.5	0.0	0.0	0.0	1.2	2.8	5.2
ankerite	0.9	0.9	2.7	0.6	1.4	1.5	0.4	0.3	0.4	0.6	0.2	1.5
pyrite	0.7	0.4	1.0	0.4	0.1	0.0	0.0	1.4	1.2	0.2	0.1	0.3
Clay minerals												
kaolinite	0.0	0.0	0.6	0.0	0.0	0.3	1.2	0.9	0.5	0.0	0.0	0.0
chlorite	14.2	12.5	18.6	9.7	10.6	9.7	11.9	9.6	11.1	17.8	14.2	13.2
1M$_d$ illite	6.0	5.4	4.2	9.8	7.9	7.6	50.6	51.3	45.6	2.7	6.3	6.3
1M illite	4.2	4.6	5.5	4.5	3.1	3.1	4.2	5.1	5.4	5.3	2.5	4.3
2M$_1$ illite	12.1	6.4	13.6	1.7	3.4	3.1	12.0	13.8	12.4	11.6	13.5	9.6
Total	95.4	98.7	100.9	97.2	100.8	100.6	99.1	98.7	95.8	101.4	94.0	100.1
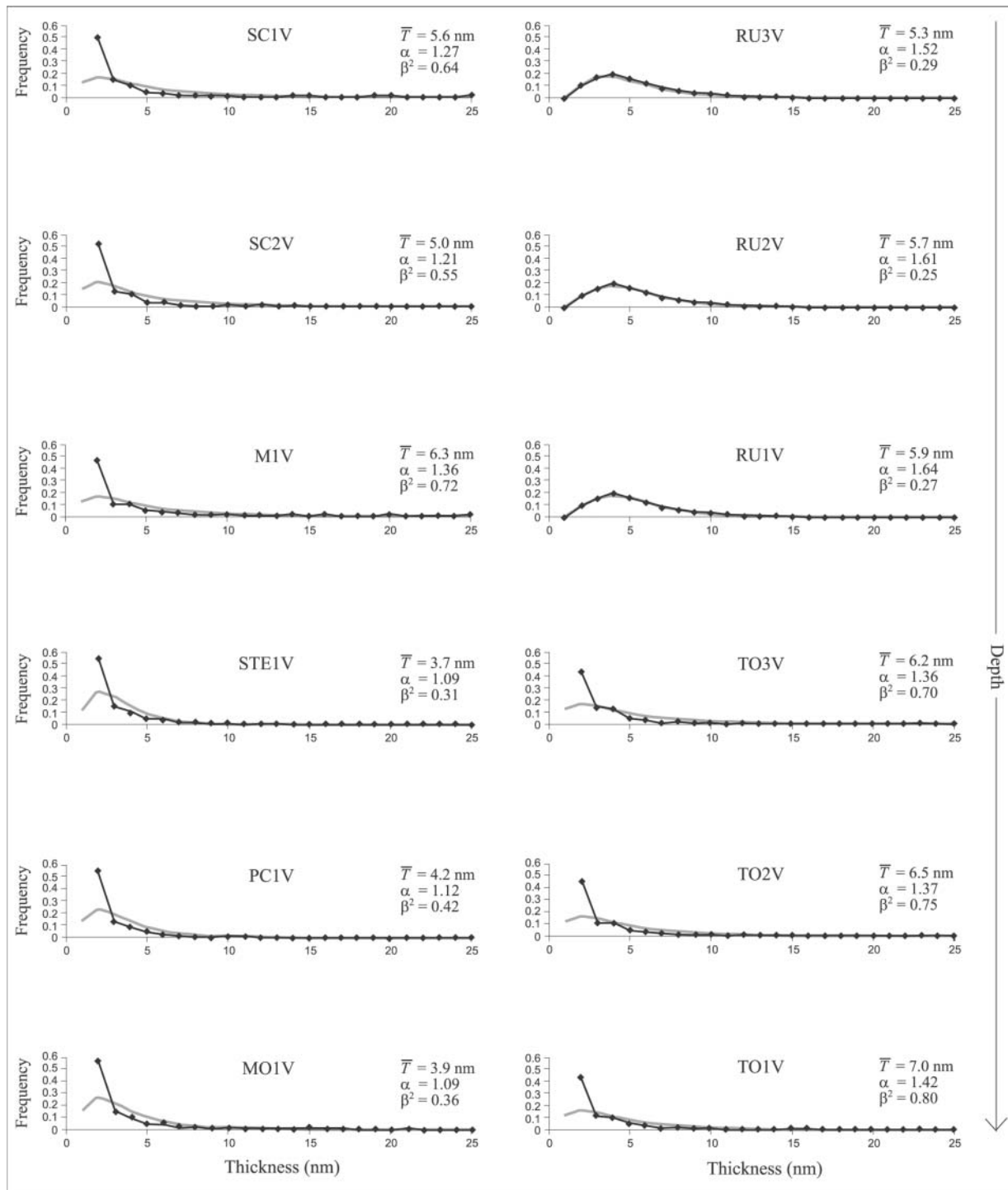
FIGURE 4. Distribution of illite crystallite thicknesses (in the studied succession) measured by the Bertaut-Warren-Averbach method using the MudMaster program. Experimental distributions are marked with diamonds. The gray line represents theoretical log-normal distributions. α is a function of the mean size and describes the mean of the natural logarithms of the crystal dimension, β^2 is a function of the shape or uniformity of the distribution and describes the variance of the natural logarithms of the crystal dimensions.

5). RAI9 is the unique sample where the R3 structure has been identified. A slight increase with depth of the illitic layers in I-S mixed layers is found in the Cervarola sandstones (from 80%

to 85%) and in the lower thrust sheets (from 80% to 85%). No discrete smectite was found.

The small increase in the percentage of the illitic layers in I-S

interstratifications is accompanied by a relatively large increase in illite mean crystallite thicknesses, from 3.7 to 7.0 nm in the 2 km thick succession of Cervarola sandstones and from 6.1 to 9.3 nm in the eastern thrust sheets. We show below that this increase in thickness is related to an increase in the $2M_1$ component in the sediments, and that this component does not participate in the mixed layering.

CRYSTAL SIZE DISTRIBUTION MODELING

We determined the relative proportions of detrital and probable diagenetic illite from crystallite thickness measurements (BWA method, using the MudMaster program of Eberl et al. 1996) by unmixing measured crystallite thickness distributions; unmixing was performed by using theoretical log-normal and/or calculated asymptotic distributions as end-members. Detrital illite was assumed to be the $2M_1$ polytype of the siliciclastic sediments, because this polytype generally is considered to form at high temperatures; diagenetic illite was assumed to be the $1M_d$ and $1M$ polytypes.

Figure 6 is an example of the unmixing of two volume-weighted crystallite size distributions: asymptotic-like (A) and log-normal-like (B). The results were obtained using the VolUnMix program, which was written as a Microsoft Excel spreadsheet (available

from the authors). The area-weighted frequencies calculated by the MudMaster analysis were automatically converted into volume-weighted frequencies in the VolUnMix program by multiplying each frequency by each thickness class. Volume-weighted frequencies then were normalized to 1.0.

The sum of the R^2 difference [(measured-calculated)^2] between the measured and the calculated CTDs was minimized by varying the proportions of the log-normal and asymptotic curves, and α and β^2 for the log-normal curves, using the Solver function in Excel.

Figure 6A shows that we needed at least two simulated asymptotic distributions and one theoretical log-normal distribution to model the experimental distribution. The best fit was obtained by trial and error using the smallest possible number of reference distributions.

The end-member components that we used to unmix the measured distributions were three asymptotic-shaped distributions calculated using the GALOPER program (phase A was simulated using 500 crystals per cycle of nucleation and growth, phase B = 333/cycle, and phase C = 250/cycle; Eberl et al., 2000) and one theoretical log-normal distribution (phase D). Unmixing always yielded a nil value for phase B.

The calculated asymptotic distributions were considered to be the diagenetic component ($1M_d$ + $1M$ polytypes) and phase D was assumed to approximate the detrital component of the mixture ($2M_1$ polytype). Furthermore, the detrital phase was constrained to have a mean thickness >10 nm (α = 2.3; β^2 = 0.16; see Uhlik et al. 2000).

The proportion of diagenetic illite can be estimated easily by calculating a weighted mean thickness for the two asymptotic crystallite thickness distributions (phase A and phase C) generally used in the unmixing procedure (e.g., proportion of phase A × mean thickness A + proportion of phase C × mean thickness C = mean diagenetic illite thickness).

Figure 6B describes the modeling of a log-normal-shape

TABLE 2. Polytype analyses (from Table 1) normalized to 1.0

Sample	$1M_d$	$1M$	$2M_1$
SC1V	0.27	0.19	0.54
SC2V	0.33	0.28	0.39
M1V	0.18	0.24	0.58
STE1V	0.61	0.28	0.11
PC1V	0.55	0.21	0.24
MO1V	0.55	0.22	0.23
RU3V	0.76	0.06	0.18
RU2V	0.73	0.07	0.20
RU1V	0.72	0.08	0.20
TO3V	0.14	0.27	0.59
TO2V	0.28	0.11	0.61
TO1V	0.30	0.22	0.48

TABLE 3. Illite crystallite thickness distributions measured by XRD for <0.2 μm (equivalent spherical diameter), <2 μm grain-size fractions, and whole-rock samples

Sample	Whole-rock			<2 μm grain-size fraction			<0.2 μm grain-size fraction		
	α	β^2	Mean thickness (nm)	α	β^2	Mean thickness (nm)	α	β^2	Mean thickness (nm)
SC1V	1.27	0.64	5.6	1.25	0.60	5.3	1.22	0.57	5.0
SC2V	1.21	0.55	5.0	1.22	0.56	5.1	1.2	0.58	5.2
M1V	1.36	0.72	6.3	1.32	0.68	5.9	1.16	0.47	4.5
STE1V	1.09	0.31	3.7	1.11	0.30	3.7	1.01	0.23	3.2
PC1V	1.12	0.42	4.2	1.12	0.35	3.9	1.03	0.23	3.2
MO1V	1.09	0.36	3.9	1.11	0.35	3.9	0.98	0.18	3.0
RU3V	1.52	0.29	5.3	1.40	0.49	5.5	1.28	0.4	4.6
RU2V	1.61	0.25	5.7	1.45	0.50	5.8	1.33	0.41	4.8
RU1V	1.64	0.27	5.9	1.53	0.38	5.6	1.41	0.33	4.9
TO3V	1.36	0.70	6.2	1.40	0.82	6.9	1.23	0.63	5.4
TO2V	1.37	0.75	6.5	1.41	0.80	7.0	1.40	0.73	6.3
TO1V	1.42	0.80	7.0	1.47	0.89	7.6	1.48	0.93	7.9
RAI9V	1.38	0.69	6.2	1.43	0.74	6.7	1.42	0.8	7.0
RAI8V	1.43	0.73	6.7	1.37	0.62	5.7	1.43	0.71	6.5
RAI7V	1.45	0.69	6.5	1.45	0.79	7.0	1.40	0.77	6.7
RAI6V	1.51	0.79	7.2	1.39	0.61	5.8	1.55	0.88	8.0
RAI5V	1.53	0.78	7.3	1.48	0.84	7.3	1.54	0.88	7.9
RAI1V	1.35	0.70	6.1	1.45	0.72	6.6	1.42	0.55	5.8
RAI4V	1.51	0.76	7.0	1.58	0.68	7.1	1.57	0.78	7.6
RAI2V	1.42	0.75	6.6	1.48	0.73	6.8	1.42	0.55	6.6
RAI3V	1.71	0.96	9.3	1.78	0.76	8.7	1.77	1.06	10.3

Note: Horizontal lines represent the different thrust sheets shown in Figure 2.
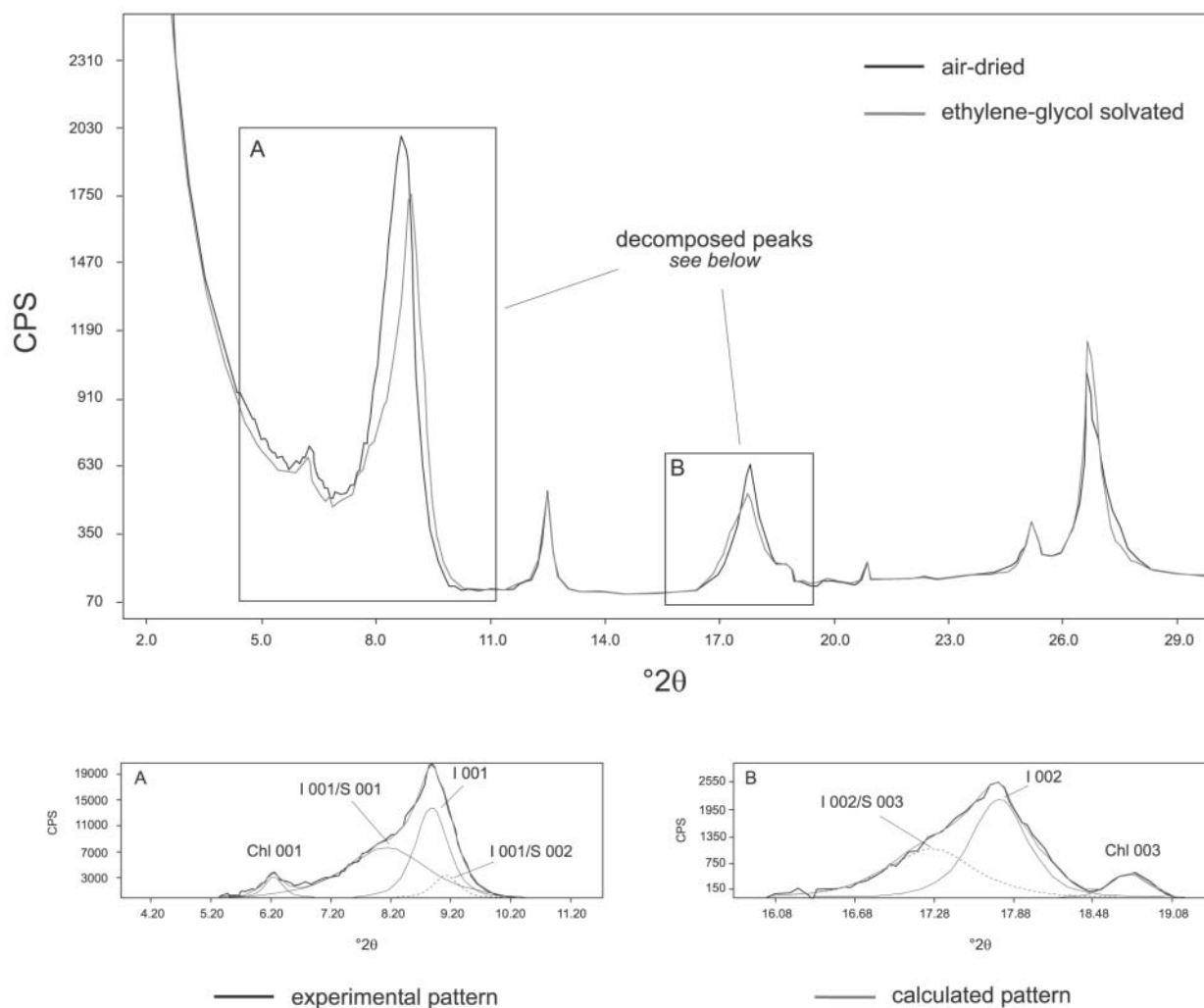
FIGURE 5. Selected XRD tracing of oriented aggregates of the RU3V sample from the <2 μm grain-size fraction showing R > 1 ordered interstratified illite (0.85)/smectite (0.15). Boxes A and B display the composite peaks decomposed through the Scintag X1 software program with a split Pearson VII function. Only I 001/S 002 and I 002/S 003 reflections were used for determining the illitic content in I-S mixed layers according to Moore and Reynolds (1997).

TABLE 4. Crystallite thickness distributions unmixing results and illitic content in the illite-smectite mixed layers

Sample	$1M_d+1M+2M_1$ mean thickness (nm)	$1M_d+1M$ mean thickness (nm)	$2M_1$ mean thickness (nm)	Proportion log-normal (VolUnMix)	Proportion $2M_1$ (Rockjock)	%I in I-S
SC1V	5.6	2.5	19.9	0.57	0.54	80
SC2V	5.0	2.5	22.3	0.46	0.39	80
M1V	6.3	2.8	21.9	0.69	0.58	80
STE1V	3.7	2.7	20.4	0.19	0.11	80
PC1V	4.2	2.6	19.7	0.37	0.24	80
MO1V	3.9	2.6	20.3	0.30	0.23	80
RU3V	5.3	5.1	18.5	0.28	0.18	85
RU2V	5.7	5.5	18.4	0.26	0.20	85
RU1V	5.9	5.7	18.0	0.25	0.20	85
TO3V	6.2	3.0	22.2	0.58	0.59	85
TO2V	6.5	2.7	22.7	0.60	0.61	80
TO1V	7.0	2.8	22.6	0.64	0.48	85

Note: The thickness of $1M_d + 1M + 2M_1$ were measured using Mudmaster. The thickness of $1M_d + 1M$, $2M_1$ and the proportion of the log-normal ($2M_1$) clays were determined using the VolUnMix program.

CTD. No asymptotic-like distributions were used to unmix the experimental curve. The best fit was obtained using two theoretical log-normal distributions: phase D was constrained to have a mean thickness >10 nm and is considered to be the detrital component of the mixture, and phase E is assumed to be the diagenetic component (α = 1.6; β² = 0.27).
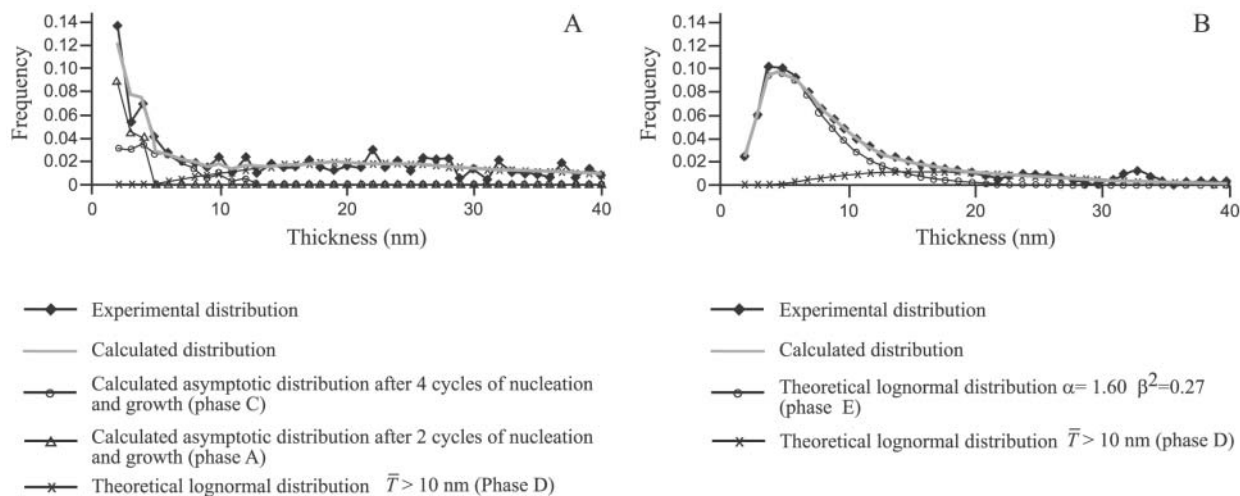
FIGURE 6. Example of unmixing (using the VolUnMix program) of two volume-weighted crystallite size distributions: an asymptotic-like (A) and a log-normal-like (B). Frequencies are normalized to 1.0.
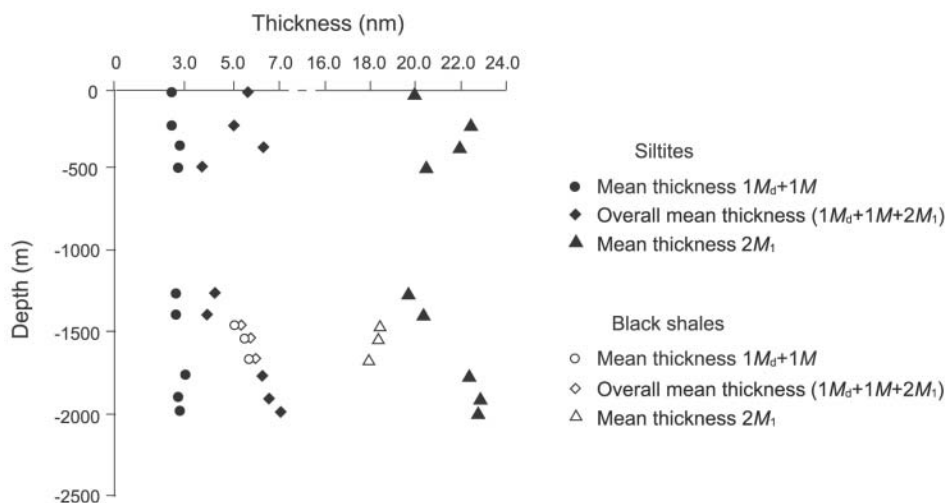

FIGURE 7. Mean thickness vs. depth diagram. Solid and open circles, triangles and diamonds represent $1M_d + 1M$, $2M_1$ and overall thicknesses of siltites and shales respectively.

RESULTS AND CONCLUSION

Modeling results were plotted in the thickness vs. depth diagram of Figure 7 and are listed in Table 4. Solid and open symbols correspond to siltites and black shales respectively. The $1M_d + 1M$ polytypes show a slight increase in mean thicknesses, ranging from 2.5 nm at the top of the succession to 3.0 nm at the bottom, whereas the $2M_1$ polytype seems to have a more accentuated trend of increasing mean thickness with depth. If both trends result from proportionate growth, then the trends can be modeled by multiplying the crystal thicknesses of the $1M_d + 1M$ and $2M_1$ illites at the top of the Cervarola sandstones by the same constant (1.1; Kile and Eberl 2003) to obtain the new thicknesses. The RU samples follow a slightly different trend because the $2M_1$ illites in these samples are thinner than those in the siltites (18 vs. 22 nm) and $1M_d + 1M$ illite crystals are 5.1 nm thick. This difference in illite thicknesses between siltites and

shales may be related to a difference in growth mechanism or rate in the shales, or to a difference in initial detrital input.

A comparison between the $2M_1$ polytype amounts found by RockJock analysis and the proportion of log-normal distributions calculated by the VolUnMix program gave comparable results with a good regression coefficient ($r^2 = 0.93$; Fig. 8), indicating that the unmixing method permits one to calculate approximately the proportion of illite polytypes, and therefore, the proportion of detrital illite, from crystallite thickness measurements. The overall illite crystallite thicknesses in the samples were found to be a function of the relative proportions of thick $2M_1$ and thin $1M_d + 1M$ illite.

The percentage of illite layers in I-S mixed layers correlates well with the mean crystallite thickness of the $1M$ ($+1M_d$) polytype, indicating that this polytype, rather than the $2M_1$ polytype, participates I-S mixed layering. In Figure 9, I-S mixed layers, simulated by having two illite particles, each 3.0 nm thick, swell
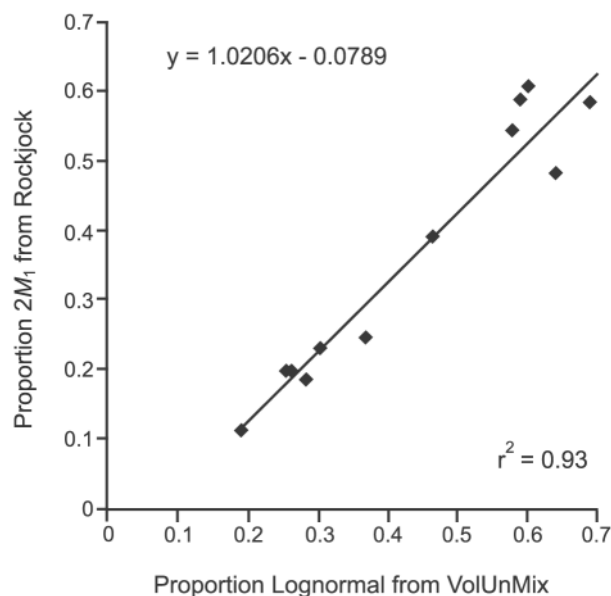
FIGURE 8. Data linear regression showing the correlation existing between the $2M_1$ polytype proportion obtained by quantitative XRD RockJock program and the $2M_1$ polytype proportion extracted by the VolUnMix program from crystallite thickness measurements (Mudmaster program).
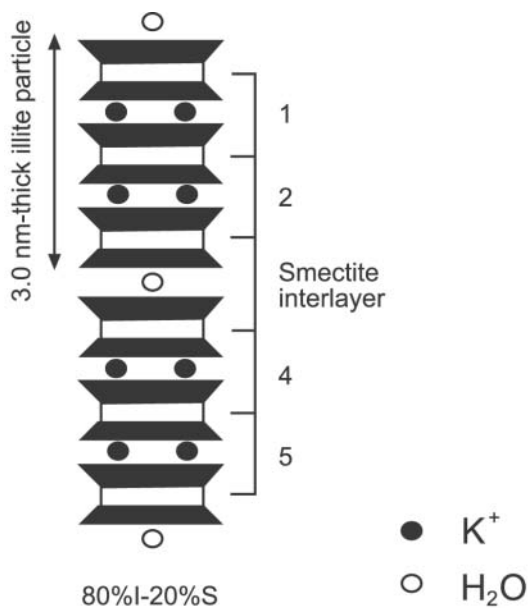

FIGURE 9. Illite-smectite mixed layer clay, with swelling at the interface between two 3 nm-thick fundamental illite particles, yielding a proportion of illite layers of 4/5 = 80% I.

at their interface and have approximately the same percentage of illite layers in I-S mixed layers as those measured by X-ray analysis. The illite content in I-S mixed layers, and the lack of R1 to R3 transition, suggest a temperature range of 100–110 and 170–180 °C (Hoffman and Hower 1979; Pollastro 1993; Árkai et al. 2002) for the studied area. Only the RAI9 sample, where R3 ordering was identified, indicates higher temperatures.

We cannot know for certain if the $2M_1$ polytype overgrows with depth at this low estimated temperatures, or if we are seeing a detrital trend (Fig. 7). A microtextural analysis performed, for example, by atomic force microscopy (AFM) could confirm or deny this hypothesis by showing euhedral or rounded $2M_1$ crystals.

ACKNOWLEDGMENTS

REFERENCES CITED

Árkai, P. (2002) Phyllosilicates in very low-grade metamorphism: transformation to micas. In A. Mottana, F.P. Sassi, J.B. Thompson, and S. Guggenheim, Eds., Micas: Crystal Chemistry and Metamorphic Petrology, 46, 463–478. Reviews in Mineralogy and Geochemistry, The Mineralogical Society of America, Washington, D.C.

Árkai, P., Fenninger, A., and Nagy G. (2002) Effect of lithology and bulk chemistry on phyllosilicate reaction progress in the low-T metamorphic Graz Paleozoic, Eastern Alps, Austria. European Journal of Mineralogy, 14, 673–686.

Boccaletti, M. (1982) Carta Strutturale dell'Appennino settentrionale, scala 1: 250.000. Progetto Finalizzato Geodinamica, Sottoprogetto 5—Modello Strutturale, Pubbl. n. 429.

Botti, F., Aldega, L., and Corrado, S. (2004) Sedimentary and tectonic burial evolution of the Northern Apennines in the Modena-Bologna area: constraints from combined stratigraphic, structural, organic matter and clay mineral data of Neogene thrust-top basins. Geodinamica Acta, 17, 185–203.

Brime, C. and Eberl, D.D. (2002) Growth mechanisms of low-grade illites based on the shapes of crystal thickness distributions. Schweizerische Mineralogische Petrographische Mitteilungen, 82, 203–209.

Burst, J.F. Jr. (1959) Post diagenetic clay mineral-environmental relationships in the Gulf Coast Eocene. Clays and Clay Minerals, 6, 327–341.

Colten-Bradley, V.A. (1987) Role of pressure in smectite dehydration-effects on geopressure and smectite to illite transformation. American Association of Petroleum Geologists Bullettin, 71, 1414–1427.

Drits, V.A., Eberl, D.D., and Środoń, J. (1998) XRD measurement of mean thickness, thickness distribution and strain for illite and illite-smectite crystallites by the Bertaut-Warren-Averbach technique. Clays and Clay Minerals, 46, 38–50.

Dudek, T., and Środoń, J. (2003) Thickness distribution of illite crystals in shales. II: origin of the distribution and the mechanism of smectite illitization in shales. Clays and Clay Minerals, 51, 529–542.

Eberl, D.D. (2003) User guide to RockJock—A program for determining quantitative mineralogy from X-ray diffraction data, 40 p. U.S. Geological Survey Open File Report OF 03-78.

Eberl, D.D., Środoń, J., Lee, M., Nadeau, P.H., and Northrup, H.R. (1987) Sericite from the Silverton caldera, Colorado: Correlation among structure, composition, origin, and particle thickness. American Mineralogist, 72, 914–934.

Eberl, D.D., Drits, V.A., Środoń, J., and Nüesch, R. (1996) MudMaster: A computer program for calculating crystallite size distributions and strain from the shapes of X-ray diffraction peaks, 44 pp. U.S. Geological Survey Open File Report 96–171.

Eberl, D.D., Nüesch, R., Šucha, V., and Tsipursky, S. (1998) Measurement of fundamental illite particle thicknesses by X-ray diffraction using PVP-10 intercalation. Clays and Clay Minerals, 46, 89–97.

Eberl, D.D., Drits, V.A, and Środoń, J. (2000) User's guide to GALOPER—a program for simulating the shapes of crystal size distributions—and associated programs, 44 pp. U.S. Geological Survey Open File Report OF 00-505.

Eberl, D.D., Środoń, J., and Drits, V.A. (2003) Comment on "Evaluation of X-ray diffraction methods for determining the crystal growth mechanisms of clay minerals in mudstones, shales and slates," by L.N. Warr and D.L. Peacor. Schweizerische Mineralogische Petrographische Mitteilungen, 83, 349–351.

Hartmann, B.H., Bodnár, K.J., Ramseyer, K., and Matter, A. (1999) Effect of Permo-Carboniferous climate on illite-smectite, Haushi group, sultanate of Oman. Clays and Clay Minerals, 47, 131–143.

Hoffman, J. and Hower, J. (1979) Clay mineral assemblages as low grade meta-morphic geothermometers: applications to the thrust faulted disturbed belt of Montana, USA. In P.A. Scholle and P.R. Schluger, Eds., Aspect of Diagenesis. SEPM Special Publication 26, 55–79, Tulsa, OK.

Hower, J., Eslinger, E.V., Hower, M.E., and Perry, E.A. (1976) Mechanism of burial metamorphism of argillaceous sediment, mineralogical and chemical evidence. Geological Society American Bullettin, 87, 725–737.

Kile, D.E. and Eberl, D.D. (2003) On the origin of size-dependent and size-in-dependent crystal growth: Influence of advection and diffusion. American Mineralogist, 88, 1514–1521.

Kotarba, M. and Środoń, J. (2000) Diagenetic evolution of crystallite thickness distribution of illitic material in Carpathian Alum shales, studied by the Ber-taut-Warren-Averbach XRD method (Mudmaster computer program). Clay Minerals, 35/2, 383–391.

Merriman, R.J. and Kemp, S.J. (1996) Clay minerals and sedimentary basin maturity. Mineralogical Society Bullettin, 111, 7–8.

Moore, D.M. and Reynolds, R.C. Jr. (1997) X-Ray Diffraction and the Identification and Analysis of Clay Minerals, 378 pp. Oxford University Press, Oxford.

Peaver, D.R. (1999) Illite and hydrocarbon exploration. Proceedings of the National Academy of Sciences, 96, 3440–3446.

Plesi, G., Daniele, G., Botti, F., and Palandri, S. (2002) Carta strutturale dell'Alto Appennino tosco-emiliano (scala 1:10.000) fra il Passo della Cisa e il Corno Alle Scale. In Cartografia Geologica—Atti del terzo seminario sulla cartografia geologica, 80–89.

Pollastro, R.M. (1990) The illite-smectite geothermometer. Concepts, methodology, and applications to basin history and hydrocarbon generation. In V.F. Nuccio and C.E. Barker, Eds., Applications of Thermal Maturity Studies to Energy Exploration. SEPM Rocky Mountain section, 1–18. Eastwood Print and Publishing, Denver, Colorado.

———. (1993) Consideration and applications of the illite/smectite geothermometer in hydrocarbon-bearing rocks of Miocene to Mississipian age. Clays and Clay Minerals, 41, 119–133.

Pollastro, R.M. and Barker, C.E. (1986) Application of clay-mineral, vitrinite reflectance, and fluid inclusion studies to the thermal and burial history of the Pindale anticline, Green River Basin, Wyoming. In D.L. Gautier, Ed., Roles of organic matter in sediment diagenesis. SEPM Special Publication, 38, 73–83.

Pytte, A.M. and Reynolds R.C. Jr. (1989) The thermal transformation of smectite to illite. In N.D. Naeser and T.H. McCulloh, Eds., Thermal History of Sedimentary Basin, p. 133–140. Springer-Verlag, New York.

Reutter, K.-J., Teichmüller, M., Teichmüller, R., and Zanzucchi, G. (1980) Le ricerche sulla carbonificazione dei frustoli vegetali nelle rocce clastiche, come contributo ai problemi di paleogeotermia e tettonica nell'Appennino settentrionale. Memorie della Società Geologica Italiana, 21, 111–126.

Reutter, K.-J., Heinitz, I., and Ensslin, R. (1991) Structural and geothermal evolution of the Modino-Cervarola Unit. Memorie Descrittive della Carta Geologica d'Italia, 46, 257–266.

Roberson, H.E. and Lahann, R.W. (1981) Smectite to illite convertion rates: effect of solution geochemistry. Clays and Clay Minerals, 29, 129–135.

Środoń, J., Drits, V.A., McCarty, D.K., Hsieh, J.C.C., and Eberl, D.D. (2001) Quantitative X-ray analysis of clay-bearing rocks from random preparations. Clays and Clay Minerals, 49, 514–528.

Tellier, K.E., Hluchy, M.M., Walker, J.R., and Reynolds, R.C. (1988) Applications of high gradient magnetic separation (HGMS) to structural and compositional studies of clay mineral mixtures. Journal of Sedimentary Petrology, 58, 761–763.

Uhlik, P., Šucha, V., Elsass, F., and Čaplovičová, M. (2000) High-resolution transmission electron microscopy of mixed-layer clays dispersed in PVP-10: A new technique to distinguish detrital and authigenic illitic material. Clay Minerals, 35, 781–789.